VIDAS ŽURAULIS, Ph.D.[1]
E-mail: vidas.zuraulis@vgtu.lt
EDGAR SOKOLOVSKIJ, Ph.D.[2]
E-mail: edgar.sokolovskij@vgtu.lt
[1] Faculty of Transport Engineering
   Transport and Logistics Competence Centre
   Vilnius Gediminas Technical University
   Saulėtekio al. 11, LT-10223 Vilnius, Lithuania
[2] Faculty of Transport Engineering
   Department of Automobile Engineering
   Vilnius Gediminas Technical University
   J. Basanavičiaus g. 28, LT-03224 Vilnius, Lithuania

VEHICLE VELOCITY RELATION TO SLIPPING TRAJECTORY CHANGE: AN OPTION FOR TRAFFIC ACCIDENT RECONSTRUCTION

ABSTRACT

In this paper, the relation of the velocity of a vehicle in the slip mode to the parameters of the tire marks on the road surface is examined. During traffic accident reconstructions, the initial velocity of a sideslipping vehicle is established according to the tire mark trajectory radius, and calculations highly depend on the directly measured parameters of the tire marks, in particular cases known as yaw marks. In this work, a developed and experimentally validated 14-degree-of-freedom mathematical model of a vehicle is used for an investigation of the relation between velocity and trajectories. The dependence of initial vehicle velocity on tire yaw mark length and trajectory radius was found as a characteristic relation. Hence, after approximation of the permanent slipping part by a polynomial, the parameters of the latter were related to vehicle velocity. The dependences were established by specific experimental tests and computer-aided simulation of the developed model.

KEY WORDS

vehicle velocity; slipping trajectory; vehicle model; traffic accident; yaw marks;

1. INTRODUCTION

An investigation of statistical data on accident rates shows that traffic accidents caused by single vehicles form 32% of the total number of accidents [1]. 70% of traffic accidents caused by single vehicles occur on suburban roads, and only 7.1% of them occur on crossroads. A study on traffic accidents carried out by experts from Germany, Italy, Netherlands, Finland, Sweden, and the United Kingdom has shown that 40% of traffic events related to vehicle yawing occur when single vehicles are involved, and almost 35% of them occur when a safe driving speed is ignored [2]. Thus, traffic events caused by single vehicles yawing from safe trajectory is a frequent traffic safety

problem, which can be tackled through an analysis of the causes of such traffic events. The methodology of traffic accident reconstruction is specified by a relation of trajectory radius change to vehicle critical speed.

Additional external forces affecting a cornering vehicle reduce its dynamic stability [3]. The role of the driver [4], which is limited in this research to keeping the vehicle control steady, is not considerably less important. If these factors are not timely assessed, the traffic accident risk increases. In a study carried out by Italian scientists Crisman and Roberti [5], a strong correlation between the radii of turns on the road and statistical data on accident rates was found: the determination coefficient is R^2=0.9 when radii of turns are under 250 m, and R^2=0.7 when radii of turns equal 250-500 m.

In traffic accident investigations, the initial velocity of a sideslipping vehicle is established according to the tire mark trajectory radius. In practice, its value highly depends on the directly measured tire mark parameters. Vehicle motion along a curvilinear trajectory is ensured by the so-called Coulomb friction. Its coefficient μ equals the ratio between the acting horizontal force and the gravity of the body [6, 7]. If a constant radius trajectory is kept, the Coulomb friction force equals the centrifugal force affecting the vehicle:

$$\mu \cdot m_v \left(g \cos \gamma \pm \frac{v_x^2}{R} \sin \gamma \right) = m_v \left(\frac{v_x^2}{R} \cos \gamma \mp g \sin \gamma \right) \qquad (1)$$

where: μ – coefficient of friction between the tire and the road surface; m_v – vehicle mass; g – acceleration of gravity (g=9.81 m/s^2); γ – angle of road superelevation; v_x – vehicle longitudinal velocity; R – trajectory radius.

From *Equation 1*, an expression for the critical velocity of a vehicle moving along a cornering trajectory is found:

$$v_{cr.} = \sqrt{\frac{Rg(\mu \pm \operatorname{tg}\gamma)}{1 \mp \mu \cdot \operatorname{tg}\gamma}} \qquad (2)$$

This formula of critical velocity (2) is applicable upon the following conditions [6]:
- The trajectory radius is established according to the tire marks on the road surface;
- The signs of the tire marks should correspond to a freely slipping vehicle;
- The road should be even, or its inclination should be assessed by calculations;
- The friction coefficient of the road surface should be established for a case when a vehicle moves in slip mode.

The first stage of the critical velocity calculation is establishing the trajectory radius according to the tire marks on the road surface. A tire mark is considered a plane curve. In the most frequently applicable method, such a curve is divided to arcs, and the radii of the latter are found by measuring the chords S_R of the arcs and the mid-perpendiculars H_R of the chords [8]:

$$R = \frac{S_R^2 + 4H_R^2}{8H_R} \qquad (3)$$

In expert practice, division of the curve to separate arcs is based on visual assessment of the curvature variation, and this may cause additional errors in the calculation of critical velocity [9]. The measurement methods have been improved, for instance, by capturing the tire marks with a camera and analyzing the images later [10]. For reproducing the real distances from the fixed images, principles of photogrammetry are applied. Images are reproduced by photographing at an angle that is as close to the right angle as possible, when the distances to the object are known; however, when estimating the angles and distances, new errors appear. By eliminating manual measurement procedures and fully applying automatic image rectification and stitching, the said errors are minimized [11].

The formula for critical velocity calculation (2) was theoretically deduced according to the movement trajectory of the vehicle center of gravity (CG). However, in practice, the tire mark trajectory radius is measured. This is partly why the application of this method of calculation is not recommended in cases of intensive yaw rate. In experimental activities [12], the calculation is carried out until the difference between the tire marks of a front wheel and a rear wheel is found to be over a fourth of the length of the vehicle base. Investigating the lateral friction coefficient values of a vehicle at different sideslip angles, American scientists [13] found that up to a sideslip angle of 60 degrees, the friction coefficient is close to its initial value. If the said value of the sideslip angle is exceeded, the friction coefficient variation (usually reduction) highly depends on thermodynamic processes in the tire contact zone as well as on vehicle control and road surface.

German scientists researched formation of tire marks and the dependence of their intensity on vehicle's dynamic parameters, the properties of the road surface, and the tires, as well as the possibilities of optical recognizability [14]. In the analysis of various tire friction values for old asphalt pavement, the primary assumption that tire marks form only when vehicle movement achieves the limit contact forces of the tires was rejected. The first marks were obtained at the friction coefficient of 0.5 in the longitudinal and lateral directions.

Another important parameter that is not directly used in *Formula 2* is the character of the longitudinal movement of the vehicle. Maximum inadequacies of calculation results were found on vehicle braking. It could be caused by a low frequency of the trajectory radius measurements. The most accurate results are obtained for an accelerating vehicle, however, they are rarely required for establishing critical velocity [6].

A cornering vehicle is also affected by additional movement resistance. It depends on driving velocity, trajectory radius, vehicle structure, tire type, tire air pressure, and the sideslip characteristics [15]. Looking for ways of reducing power consumption, specialists from the vehicle manufacturer Toyota found that at lateral acceleration of 0.4 g vehicle cornering resistance doubles. [16]. Therefore, when analyzing the relation between vehicle trajectory and velocity, it should be noted that the radius is variable, even if the driving conditions (such as driver's actions, different pavement or wind properties) are neglected.

Improvements to the measurement methods for cornering vehicle parameters that enable to establish whether the driver could avoid the traffic accident fosters objective expert activities that are highly important for practical investigation of traffic events [17]. In this paper, the relation between the velocities of a cornering vehicle and the parameters of the slipping trajectory is discussed. The methods applicable to traffic event investigations are more closely defined according to trajectory variations. To that end, a vehicle mathematical model validated by experimental tests is used.

2. VEHICLE MODEL

By analyzing vehicle movement and its regularities and taking into account the character of the movement, mathematical models of vehicles are developed. The chosen model enables to simplify the total system and work in a proper environment while avoiding assessment of less important parameters or accepting them as known [18]. In such a case, expensive experimental tests are limited to the extent sufficient for validating the model.
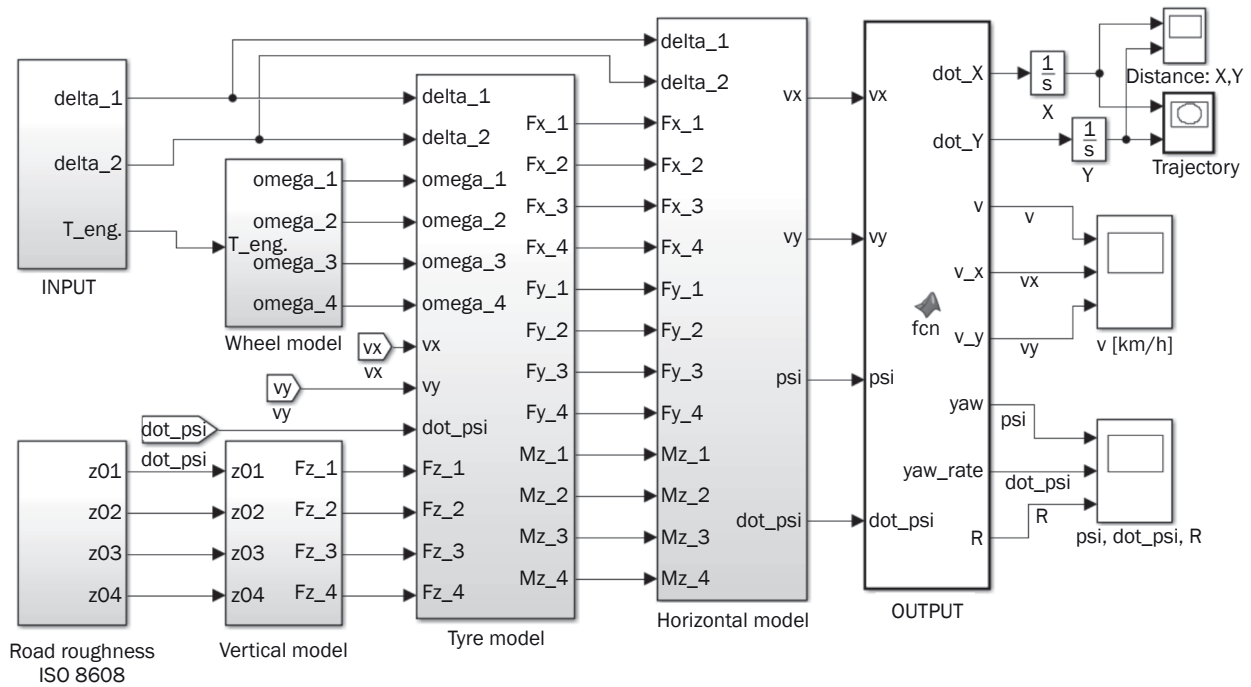
Figure 1 – General view of 14-DOF vehicle model in MATLAB/Simulink environment

The MATLAB/Simulink package with graphical and textual programming forms is used for vehicle movement simulation. The developed 14-degree-of-freedom (DOF) vehicle model enables analyzing vehicle motion depending on the input parameters of the model, such as steering angle and the engine's tractive effort torque as well as the road parameters. The two first parameters serve as the driver's actions. The roughness height and surface adhesion properties were selected with respect to the road. The entire vehicle model consists of the following interrelated components: vertical model, wheel model, tire model, and horizontal model. The model components and their relations with the input and output elements in the software environment are shown in *Figure 1*. The vehicle model was constructed using different sources but validated as an option for accident reconstruction methodology.

The engine's tractive effort torque is recalculated (according to the inertial and resistance forces) into the angular velocities of the driving wheels usable for calculation of longitudinal slip-ratio in the tire model. The input of the wheels' steering angles in the tire model is used for calculation of the sideslip angle. In the vertical model, the normal forces of the wheels are calculated based on the entered road roughness value for each wheel and the longitudinal and lateral accelerations that cause oscillations of sprung mass. The established wheel slips and normal forces are used for generation of longitudinal and lateral contact forces. The aligning moments in the tire model and the above-listed parameters are entered in the equations of the longitudinal, lateral, and cornering movements of the vehicle, taking into account the steering wheels'

cornering angles and the position of the vehicle. The parameters required for establishing vehicle velocity and trajectory are obtained in the horizontal model.

2.1 Vertical model

The vertical model describes the movement of individual masses depending on road roughness as well as the acting body's longitudinal and lateral forces. In this model, the vehicle body, including the systems, the driver, the passengers, or the cargo, is usually named the sprung mass, and the wheels with the related systems (brakes, a part of the suspension, and the transmission) are named the unsprung masses.

The vertical model is a 7-DOF model: the vertical travel of the four unsprung masses $z_{1,2,3,4}$ and the vertical travel of the sprung mass z as well as oscillations around the longitudinal and lateral axis of the vehicle, respectively roll φ and pitch θ [19].

In the calculation, the vertical model is considered as a system of dynamic vibrations. The system of coordinates fixed in the vehicle CG conforms to the standard ISO 8855 [20]. The dynamic system's equations of motion are written upon applying Lagrange second-order equations:

$$m\ddot{z} = -c_1\dot{z}_{z\text{-}1} - c_2\dot{z}_{z\text{-}2} - c_3\dot{z}_{z\text{-}3} - c_4\dot{z}_{z\text{-}4}$$
$$- k_1z_{z\text{-}1} - k_2z_{z\text{-}2} - k_3z_{z\text{-}3} - k_4z_{z\text{-}4} - mg \tag{4}$$

$$I_x\ddot{\varphi} = -c_1a_1\dot{z}_{z\text{-}1} - c_2a_2\dot{z}_{z\text{-}2} - c_3a_1\dot{z}_{z\text{-}3} - c_4a_2\dot{z}_{z\text{-}4}$$
$$- k_1a_1z_{z\text{-}1} - k_2a_2z_{z\text{-}2} - k_3a_1z_{z\text{-}3} - k_4a_2z_{z\text{-}4}$$
$$- ma_y \cdot h_\varphi \cdot \cos\varphi + mg \cdot h_\varphi \cdot \sin\varphi \tag{5}$$

$$I_y\ddot{\theta} = -c_1b_1\dot{z}_{z\text{-}1} - c_2b_1\dot{z}_{z\text{-}2} - c_3b_2\dot{z}_{z\text{-}3} - c_4b_2\dot{z}_{z\text{-}4}$$
$$- k_1b_1z_{z\text{-}1} - k_2b_1z_{z\text{-}2} - k_3b_2z_{z\text{-}3} - k_4b_2z_{z\text{-}4}$$
$$- -ma_x \cdot h_\theta \cdot \cos\theta - mg \cdot h_\theta \cdot \sin\theta \tag{6}$$

$$m_1\ddot{z}_1 = c_1\dot{z}_{z\text{-}1} + k_1 z_{z\text{-}1} - c_{t1}\dot{z}_{1\text{-}0} - k_{t1}z_{1\text{-}0} - m_1 g \tag{7}$$

$$m_2\ddot{z}_2 = c_2\dot{z}_{z\text{-}2} + k_2 z_{z\text{-}2} - c_{t2}\dot{z}_{2\text{-}0} - k_{t2}z_{2\text{-}0} - m_2 g \tag{8}$$

$$m_3\ddot{z}_3 = c_3\dot{z}_{z\text{-}3} + k_3 z_{z\text{-}3} - c_{t3}\dot{z}_{3\text{-}0} - k_{t3}z_{3\text{-}0} - m_3 g \tag{9}$$

$$m_4\ddot{z}_4 = c_4\dot{z}_{z\text{-}4} + k_4 z_{z\text{-}4} - c_{t4}\dot{z}_{4\text{-}0} - k_{t4}z_{4\text{-}0} - m_4 g \tag{10}$$

where: m – vehicle sprung mass; m_i – unsprung mass; i – the index of the vehicle unsprung mass or its wheel or its suspension (1 – front left, 2 – front right, 3 – rear left, 4 – rear right); I_x – roll moment of inertia; I_y – pitch moment of inertia; h_φ – the distance from the vehicle CG to the roll axis; h_θ – the distance from the vehicle CG to the pitch axis; c_i – suspension damping coefficient; k_i – suspension stiffness coefficient; c_{ti} – tire damping coefficient; k_{ti} – tire stiffness coefficient; g – acceleration of gravity (9.81 m/s2); $z_{z\text{-}i}$, $z_{i\text{-}0}$ – the displacements of the vehicle suspension and tires, respectively:

$$z_{z\text{-}1,z\text{-}3} = z - z_{1,3} + a_1\varphi \mp b_{1,2}\theta \tag{11}$$

$$z_{z\text{-}2,z\text{-}4} = z - z_{2,4} + a_2\varphi \mp b_{1,2}\theta \tag{12}$$

$$z_{i\text{-}0} = z_i - z_{0i} \tag{13}$$

where: z_{0i} – the vertical travel of a relevant wheel of the vehicle caused by road roughness; $a_{1/2}$ – lateral distance from vehicle CG to left/right wheel; $b_{1/2}$ – longitudinal distance from vehicle CG to front/rear wheel.

The classification of road surface profile unevenness is provided in the international standard ISO 8608 [21]. For this classification, spatial power spectral density (spatial PSD) is used. This value shows roughness reduction over wavelength increase, and it is calculated as follows [22]:

$$G_q(n) = G_q(n_o)\left(\frac{n}{n_o}\right)^{-\omega} \tag{14}$$

where: n – spatial frequency (n_o=0.1 cycles/m); ω – road surface waviness ($1.75 \le \omega \le 2.25$); $G_q(n_o)$ – degree of road surface roughness.

In the vertical model, road roughness height is used. Its variation at a time moment is shown by the following expression [23]:

$$\dot{z}_o(t) = -2\pi v_{xi}(t)n_o z_o(t) + w(t)\sqrt{G_q(n_o)v_{xi}(t)} \tag{15}$$

where: $v_{xi}(t)$ – the longitudinal velocity of a relevant wheel; $w(t)$ – the constant spectral density.

The dynamic normal forces established in the vertical model are used in the tire model for calculation of contact forces.

2.2 Wheel model

The wheel model is used for establishing the angular velocities of wheels depending on the torsional torque transferred from the engine via the transmission or braking moment. Each wheel adds one DOF to the vehicle model. In addition, the contact forces generated in the tire model and the rolling resistance are used in the expression of this model [24]:

$$I_{wi}\dot{\omega}_i = T_{eng.}i_{tr.}\eta_{tr.} - T_{br.} - F_{xi}r_{di} - F_{r.r.i}r_{di} \tag{16}$$

where: $T_{eng.}$ – engine torque; $i_{tr.}$ – transmission ratio; $\eta_{tr.}$ – transmission efficiency; $T_{br.}$ – the braking moment applied to a wheel in case of its braking; F_x – longitudinal contact force generated in the tire model; r_d – dynamic radius of a wheel; I_w – rotational moment of inertia of a wheel; $F_{r.r.}$ – rolling resistance of a respective wheel:

$$F_{r.r.i} = F_{zi}\cos\alpha_{road}f_o(1 + Av_x^2) \tag{17}$$

where: F_z – normal force of a wheel established in the vertical model; α_{road} – longitudinal road inclination angle; f_o – coefficient of rolling resistance; A – empirical rolling resistance correction coefficient [25]; v_x –vehicle longitudinal velocity obtained in the horizontal model.

An individual calculation of angular velocities for each wheel ensures a proportional distribution of the torque transferred from the engine. In the modeling of the chosen vehicle, the engine torque is not used for the rear wheels.

2.3 Tire model

Scientists L. Segel, H. Dugoff, and P. Favcher developed a tire model that assesses: normal force, longitudinal slip-ratio, stiffness of longitudinal and lateral contact, and friction coefficient. USA scientist Dugoff formulated the primary expressions for the model, then it was improved and supplemented with varying normal forces and aligning moments. In the tire model developed by the Highway Safety Research Institute (HSRI), the formulated mathematical expressions enable rather exact establishing of the contact forces and the aligning moment using comparatively few parameters and experimental tests. This model is also applicable in expert calculations for traffic events [26]. The physical concept of the model is based on the calculation of the tire longitudinal and lateral contact forces according to the contact zone, where deformed slipping and interacting with the road areas are singled out. The contact forces are obtained based on establishing an interacting area and its relation with the sideslip angle.

The contact forces of a tire are calculated according to the values of the longitudinal slip ratio and sideslip angle [27]:

$$s_i = \frac{\omega_i r_d - v_i\cos\alpha_i}{\max(\omega_i r_d, v_i\cos\alpha_i)} \tag{18}$$

where: ω – wheel angular velocity; r_d – dynamic wheel radius; v_i –longitudinal wheel velocity; i – index of a respective wheel.

The longitudinal velocity of a respective wheel is:

$$v_{1,2} = v \mp \dot{\psi} a_{1,2} \cos\beta + \dot{\psi} b_1 \sin\beta \qquad (19)$$

$$v_{3,4} = v \mp \dot{\psi} a_{1,2} \cos\beta - \dot{\psi} b_2 \sin\beta \qquad (20)$$

where: v – vehicle velocity in the CG; β – vehicle body sideslip angle in the CG:

$$\beta = \arctan\left(\frac{v_y}{v_x}\right) \qquad (21)$$

where $v_{x,y}$ – vehicle velocity in the CG in longitudinal and lateral direction established in the horizontal model.

The tire sideslip angle according to components of velocity is:

$$\alpha_{1,2} = \delta_{1,2} - \arctan\left(\frac{v \sin\beta + b_1 \dot{\psi} \sin\beta}{v \cos\beta \mp a_{1,2} \dot{\psi} \cos\beta}\right) \qquad (22)$$

$$\alpha_{3,4} = -\arctan\left(\frac{v \sin\beta - b_2 \dot{\psi} \sin\beta}{v \cos\beta \mp a_{1,2} \dot{\psi} \cos\beta}\right) \qquad (23)$$

where δ_i – wheel steering angle (model input value).

If the values of the slip-ratio and sideslip angle of each wheel are known, the instantaneous adhesion of tire with the road surface is expressed as follows:

$$\mu_i = \mu_{max}\left(1 - A_s \cdot \omega_i r_d \sqrt{s_i^2 + \tan^2\alpha_i}\right) \qquad (24)$$

where: μ_{max} – maximal road friction coefficient; A_s – coefficient assessing the reduction of friction coefficient (0.0115).

The dynamic normal forces of wheels established in the vertical model are used in the calculation of the parameter expressing the tire slip value:

$$H_{si} = \frac{\sqrt{(K_s s_i)^2 (K_\alpha \tan\alpha_i)^2}}{\mu_i F_{zi}(1 - s_i)} \qquad (25)$$

where: K_s – longitudinal tire stiffness; K_α – tire side stiffness.

If the tire slip is not significant, it is considered that only molecular interaction (adhesion) takes place in the contact zone between the surfaces, and the variation of the longitudinal and lateral contact forces of the tire caused by the slip is linear, and the slippage parameter $H_s \leq 0.5$ [28]. On increase of the longitudinal and lateral tire slip, one part of the adhesive contact zone is considered as slippage zone, while the other part is not slipping. The friction coefficient μ decreases, and the slippage parameter H_s increases and exceeds the limit of 0.5. Therefore, depending on slippage intensity, the contact forces in the longitudinal and lateral direction, respectively, are established according to the following expressions [29]:

$$F_{xi} = \begin{cases} K_s \dfrac{s_i}{1 - s_i}, & \text{when } H_{si} \leq 0.5, \\[2mm] K_s \dfrac{s_i}{1 - s_i} \cdot \dfrac{H_{si} - 0.25}{H_{si}^2}, & \text{when } H_{si} > 0.5, \end{cases} \qquad (26)$$

$$F_{yi} = \begin{cases} K_\alpha \dfrac{\tan\alpha_i}{1 - s_i}, & \text{when } H_{si} \leq 0.5, \\[2mm] K_\alpha \dfrac{\tan\alpha_i}{1 - s_i} \cdot \dfrac{H_{si} - 0.25}{H_{si}^2}, & \text{when } H_{si} > 0.5, \end{cases} \qquad (27)$$

When simulating a gentle and smooth maneuver, the tire aligning moment usually is not used [25]. However, if sudden maneuvers are carried out or considerable slip of the vehicle is provoked, the moment should be assessed:

$$M_{zi} = F_{yi} t_y - F_{xi} t_x \qquad (28)$$

where: $t_{y,x}$ – the arms of pneumatic stretching force on the tire contact surface in the longitudinal and lateral direction, respectively [29]:

$$t_x = \begin{cases} \dfrac{1}{3} l_{const.}, & \text{when } H_{si} \leq 0.5, \\[3mm] l_{const.}\left(\dfrac{12 - \dfrac{1}{H_{si}^2}}{12 - \dfrac{3}{H_{si}^2}} - 1\right), & \text{when } H_{si} > 0.5, \end{cases} \qquad (29)$$

$$t_y = \begin{cases} \dfrac{1}{3} l_{const.} \tan\alpha_i + \dfrac{F_{yi}}{K_y}, & \text{when } H_{si} \leq 0.5, \\[3mm] \dfrac{l_{const.}\left(H_{si} - \dfrac{1}{3}\right)}{H_{si}\left(H_{si} - \dfrac{1}{4}\right)} \tan\alpha_i + \dfrac{F_{yi}}{K_y}, & \text{when } H_{si} > 0.5, \end{cases} \qquad (30)$$

where: $l_{const.}$ – length of tire contact path; K_y – lateral tire stiffness.

The contact forces and moments established in the tire model for each wheel are further used in the horizontal model.

2.4 Horizontal model

The horizontal model describes the movement of a vehicle as an integral body and has 3 DOF: movement in the longitudinal and lateral direction v_x, v_y, as well as yaw rotation around the vertical axis ψ. The equations of the model's longitudinal and lateral motion are formulated adjusting the forces in the respective directions [30]:

$$m_{total} a_x = F_{x1} \cos\delta_1 - F_{y1} \sin\delta_1 + F_{x2} \cos\delta_2 \\ - F_{y2} \sin\delta_2 + F_{x3} + F_{x4} - F_{resist.} \qquad (31)$$

$$m_{total} a_y = F_{x1} \sin\delta_1 + F_{y1} \cos\delta_1 \\ + F_{x2} \sin\delta_2 - F_{y2} s \cos\delta_2 + F_{y3} + F_{y4} \qquad (32)$$

where: m_{total} – total vehicle mass; a_x / a_y – acceleration acting on the vehicle along the longitudinal/lateral axis; F_x / F_y – contact force acting on the respective wheel tire along the longitudinal/lateral axis; δ_i – steering angle of the respective steering wheel; $F_{resist.}$ – vehicle movement resistance forces.

The equation for the rotation of the model around the vertical axis is formed upon establishing the moments affecting the CG of the vehicle:

$$I_z \ddot{\psi} = (F_{x1} \sin\delta_1 + F_{y1} \cos\delta_1 + F_{x2} \sin\delta_2 + F_{y2} \cos\delta_2)b_1 \\ - (F_{y3} + F_{y4})b_2 - (F_{x1} \cos\delta_1 - F_{y1} \sin\delta_1)a_1 \\ + (F_{x2} \cos\delta_2 + F_{y2} \sin\delta_2)a_2 - F_{x3} a_1 + F_{x4} a_2 + \sum_{i=1}^{4} M_{zi} \qquad (33)$$

The acceleration affecting the vehicle along the longitudinal axis and the component of the lateral acceleration related to rotation around the vertical axis are the input data in the vertical model that cause oscillations and transfers of support reactions due to maneuvering. The accelerations along the longitudinal/lateral axis are expressed by the change of velocity and the velocity of rotation around the vertical axis as follows:

$$a_{x,y} = \dot{v}_{x,y} \mp \dot{\psi} v_{y,x} \tag{34}$$

The total resistance force affecting the vehicle consists of the air resistance force and the slope resistance force:

$$F_{resist.} = F_w + F_{road} = \frac{v_x^2}{2} \rho_{air} c_w A_f + m_{total} g \sin \alpha_{road} \tag{35}$$

where: ρ_{air} – mass density of the air; c_w – vehicle drag coefficient; A_f – characteristic frontal area of the vehicle; α_{road} – longitudinal road inclination angle.

The vehicle velocity components in the longitudinal and lateral direction as well as yaw rate are established from the model of horizontal forces. According to the velocity values and sideslip angle of the vehicle obtained in the tire model, the following cornering vehicle parameters are found: the position coordinates X and Y as well as the trajectory radius R:

$$X = \int \left(\cos(\beta + \psi) \cdot v_x - \sin(\beta + \psi) \cdot v_y \right) dt \tag{36}$$

$$Y = \int \left(\sin(\beta + \psi) \cdot v_x + \cos(\beta + \psi) \cdot v_y \right) dt \tag{37}$$

$$R = \frac{v_x}{\dot{\psi}} \tag{38}$$

The velocity established in the horizontal model is used for the formation of input data on the road roughness (*Equation 15*) and calculation of slippage parameters in the tire model (*Equations 18, 22, 23*). The longitudinal and lateral accelerations cause vibrations of the sprung mass in the vertical forces model. Thus, the horizontal forces model unites all the parts of the general 14-DOF mathematical model of the vehicle, assesses the main movement resistance forces and the input data on steered wheels during vehicle cornering and derives the trajectory and radius parameters required for the further paper analysis.

3. EXPERIMENTAL PROCEDURE AND MODEL VALIDATION

Prior to further application of the mathematical vehicle model, its validation takes place. During the experimental test, when the vehicle achieves a constant velocity, the steered wheels are turned at a speed not lower than 3°/s. Such maneuvering simulates a sudden cornering or a change of vehicle movement trajectory. On changing the trajectory, the vehicle is allowed to move freely while maintaining the same steering angle, the same gear, with no acceleration or braking until the vehicle affected by increased resistance forces naturally decelerates and is fully stopped. No actions causing additional slipping or stabilization of the vehicle by the steering wheel and other controls were carried out. The road surface during the tests was dry asphalt ($\mu \approx 0.85$); its smoothness was close to the class C according to ISO 8608 [21]. The parameters conforming to the said class are included in the input data for the vertical model.

For the experimental test, light vehicle *Toyota Avensis* was used. Its dynamic parameters were fixed using certified measurement equipment from *Corrsys-Datron*, a member of the *Kistler Group* [31]. The inertial measurement unit (IMU) *TANZ-3* was installed in the vehicle, close to the CG. At the front of the vehicle, an optical movement sensor along the longitudinal and lateral axes and the yaw angle measurement sensor *Correvit S-350 Aqua* were installed. The steering wheel angles were measured by the *Kistler RV-4 system*. The data from the sensors were synchronously recorded at 200 Hz using the data acquisition system *DAS-3* (from *Corrsys-Datron*) fixed inside the vehicle. The position and trajectory of the vehicle were fixed by a GPS sensor mounted on the roof of the vehicle. The GPS sensor data was recorded by the *DL1* device (from the company *Race Technology*), processed, and converted by the *RT Analysis software*. The accuracy of the used sensors was up to ±0.2%.

For the model validation, 20 cornering trajectory maneuvers were performed. For each test, the initial velocity at the beginning of tire mark formation and trajectory radius variation in the course of vehicle slippage are shown in *Figure 2*. Extension to a wider speed range is always possible. The plot formed on the basis of the experimental data (*Figure 2*) shows a considerable dispersion of the vehicle trajectory radius values depending on the initial velocity fixed at the beginning of tire mark formation. The quantile field of the dependence between the trajectory radius and the initial velocity varies from 6.5 m to 15.5 m, and the range of quantile outliers in any case is more oriented towards the positive direction of the curve – this attests to an increase of the marginal values of the trajectory radius, i.e., straightening of the trajectory. The observed growing trend of the middle trajectory radius is not considerable because the sample of initial velocity values is 4.58 m/s.

For a detailed analysis of the most intensive fragment of the cornering trajectory, the dependence between the driving velocity and the trajectory radius was chosen (*Figure 3*). It is notable that the chosen fragment is limited by the trajectory radius ($R<80$ m): if its value is exceeded in certain cases, the movement is already stable and predictable (the measured sideslip angle < 2°, and the tire marks are not observed). In addition, the chosen fragment is limited by the
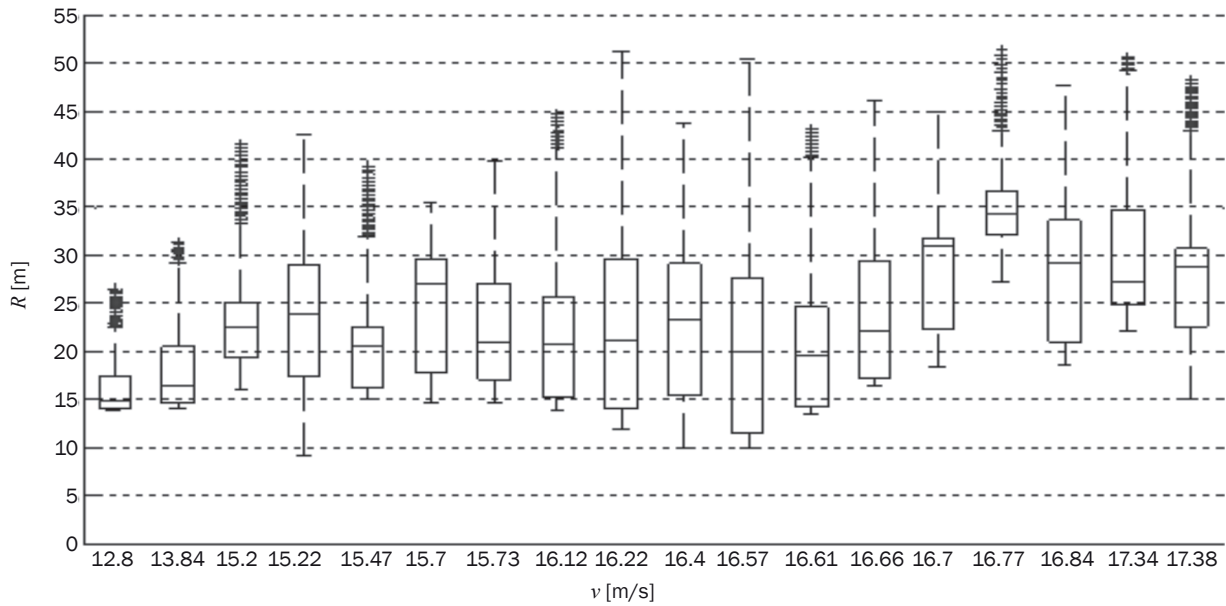
Figure 2 – The dispersion of trajectory radius values over initial velocity
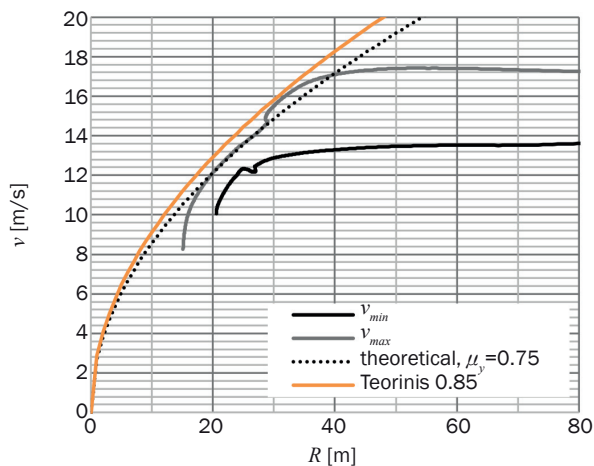

Figure 3 – The dependence between the vehicle velocity and trajectory radius during the cornering maneuvers

moment when the radius begins to suddenly increase at the end of the maneuver – the velocity considerably decreases before the vehicle stops, and its trajectory is straightened (actions of the driver).

The dotted line (*Figure 3*) shows the theoretical dependence according to *Formula 2*, when the lateral tire-road friction coefficient equals 0.75 ($\mu_y=0.9\mu_x$). It can be seen from the curve that the theoretical *R-v* dependence exactly conforms to the experimental dependences in a narrow range only (*R*–from 20 to 30 m). If the velocity is insufficient, i.e., the critical limit of tire contact forces is not achieved (the case of v_{min}), the *R-v* dependence does not achieve the theoretical curve. This means that cornering movement is stable and controlled by the driver. If the initial velocity is too high for the chosen trajectory (the case of v_{max}), it is observed that the theoretical dependence is exceeded.

It may be supposed that the vehicle was slipping at a certain moment of movement, and the trajectory of the movement did not conform to the trajectory limited by the contact forces. Thus, while analyzing real cornering movement cases, the theoretical dependence between the trajectory radius and the friction coefficient may be applied in a narrow range limited by movement parameters. Because of that, it is important to foresee the *R-v* dependence in a broader range of velocities.

For slip mode cornering, more precise methods of velocity forecasting should be applied. In this case, slip mode movement is considered to be the movement when tire yaw marks appear. When the experimental dependences achieve and exceed the theoretical curve, the zone shown in *Figure 3* coincides with the sideslip tire marks obtained during the experiments. However, no tire marks were observed in the case of insufficient velocity v_{min}.

The experimental tests on vehicle cornering movement in slip mode were carried out on dry asphalt pavement ($\mu_x=0.85$), and visual observation of tire marks revealed that they are visible from the lateral acceleration of 7 m/s² affecting the vehicle. This means that from this limit the tires achieve peak contact forces, and rubber particles separate from the tires and remain on the road surface thus forming the tire marks. Such separation of rubber particles is predetermined by contact temperature increase (caused by friction) and tangential tensions (caused by vertical and lateral forces). In each case, the road pavement may cause a different friction coefficient. The surface structure and micro-roughness are the conditions for rubber particles adhesion. If the road pavement is uneven, a tire mark may be discontinuous, and

extraneous particles (such as fine-grained macadam, grit, or impurities) may cause mechanical scratches on the pavement instead of tire marks.

Hence, the tire mark trajectory changes show that for further analysis the radius and velocity values should be related with the tire mark length S. Applicable measurement equipment provides an opportunity to relate the lateral acceleration affecting the vehicle with the road surface affected by carrying out the measurements with two individual devices (GPS and WPT). As noted before during the dry asphalt pavement test, exceeding the acceleration of 7 m/s² means that the tire mark length is S.

Presenting the dependence between the tire mark length, the trajectory radius, and the velocity (*S-R-v* dependence) in a mutual system of coordinates makes it convenient to assess the conformity of the vehicle mathematical model with the results of the experimental tests (*Figure 4*). Here, the horizontal base-plane conforms to the *S-R-v* dependence obtained by simulations of the mathematical model for cornering

trajectory maneuvers (*Figure 5*). The absolute values of residual errors of the experimental tests are graphically shown as black curves (*Figure 4*). The established maximum absolute velocity errors do not exceed 2.5 m/s, and the root mean square error (RMSE) equals 0.475. For predicting the initial velocity of the vehicle, the primary slipping phase, when free sideslipping without braking or acceleration takes place until the velocity reduces because of kinetic energy losses, is the most important. In this phase ($S<30$ m), the absolute velocity errors do not exceed 1.5 m/s.

Therefore, the *S-R-v* dependence, formed in the course of the mathematical simulation and validated by the experimental test data, is fit for predicting the initial velocity of a vehicle of the investigated class according to the known parameters of tire mark length S and trajectory radius R. The mathematical simulation enabled extending the range of investigated velocities up to 50 m/s, and carrying out the same via an experiment would require special conditions.
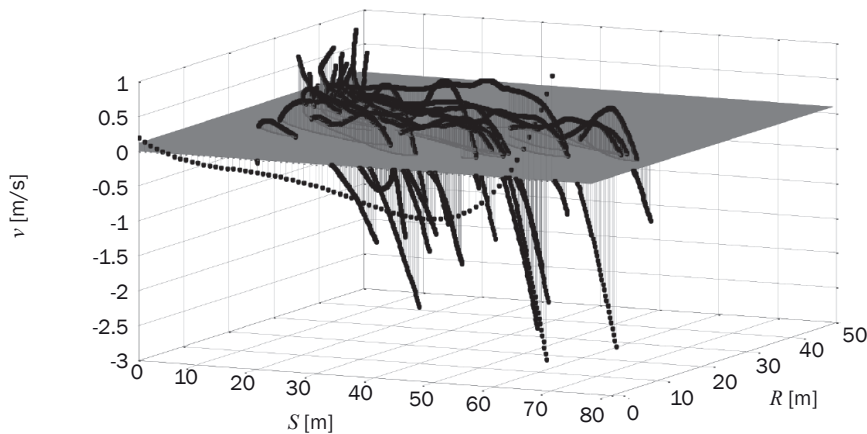

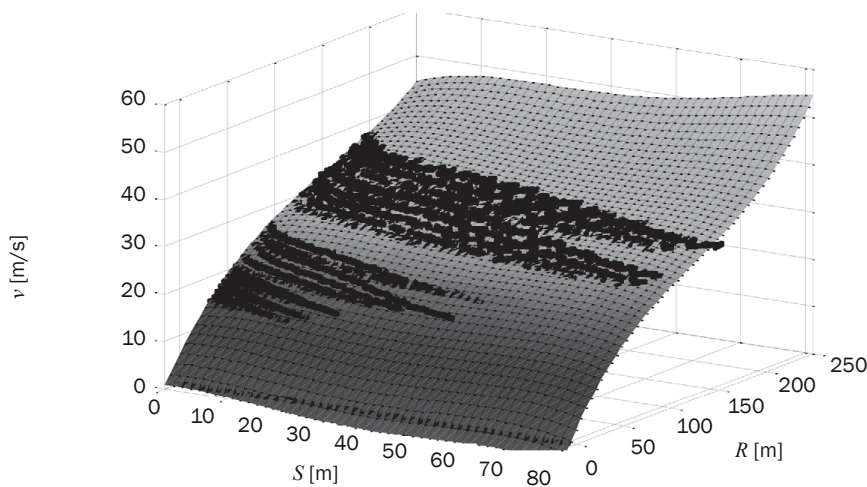*Figure 4 – Residual errors of regression model experimental tests*

Figure 5 – The S-R-v dependence curve obtained by mathematical simulation (R^2=0.97)

The surface formed upon applying regression analysis (*Figure 5*) shows that velocity v values increase when the tire mark length S increases. This means that if the trajectory radius does not reduce under the tire mark formation conditions, the velocity should increase, i.e., a reserve of kinetic energy is required to support slipping. Under real conditions, such cases are rare (slipping due to increased engine torsion torque), and this is confirmed by the downward black curves obtained in course of the mathematical simulation. They show a gradual natural reduction of the velocity (loss of kinetic energy) when the tire mark formation conditions remain.

4. ANALYSIS OF SLIPPING TRAJECTORY CHANGE

Trajectory approximation obtained by photogrammetry [11] is appropriate for formation of a characteristic curve of maximum possible accuracy according to the preset points of coordination of the tire marks. For establishing the trajectory radius, the derivative of the polynomial that approximates the trajectory is calculated; the said derivative conforms to a tangent of the curve. The perpendicular of this tangent until the point of intersection with the perpendicular of the tangent of another point of the trajectory is considered an instantaneous radius.

For establishing radius changes, the tire mark length was not analyzed in total. The initial part and the end part are rejected, and the middle part of the trajectory radius variation is much more continuous, i.e., variation takes place in a narrow radius range. In the course of experiments, it was found that, taking the accuracy into account, the optimum approximation should involve 50% of the internal part of the tire mark length. A smaller part of its length will not improve the accuracy, and if this part is increased, the variation of radius values will become more intensive (*Figure 6*). In case of an approximation of a part of the tire mark length, the radius variation curve is not sensitive to the polynomial degree, therefore using a third-degree polynomial is sufficient.

After establishing the variation of slipping trajectory radius in respect of a tire mark by regression analysis, a linear dependence is observed, i.e., the radius reduces continuously in respect of the slipping path. The said trend comes to light when the radius variation is established from the steady part of the slip mark distance (*Figure 6*). Such a link should be related to a
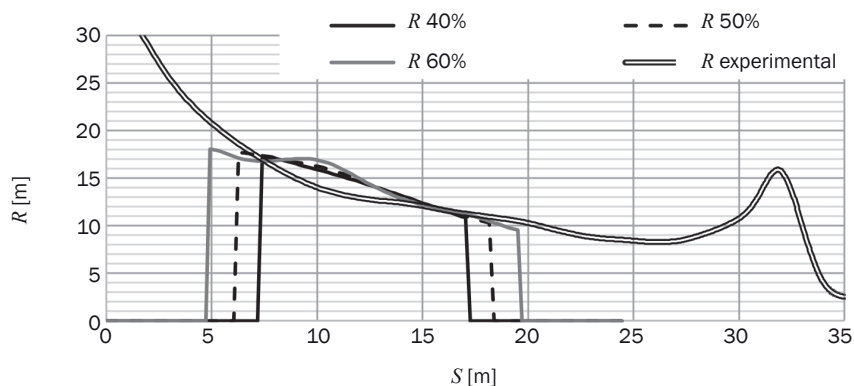

Figure 6 – Establishing the trajectory radius by approximation according to a part of the tire mark length
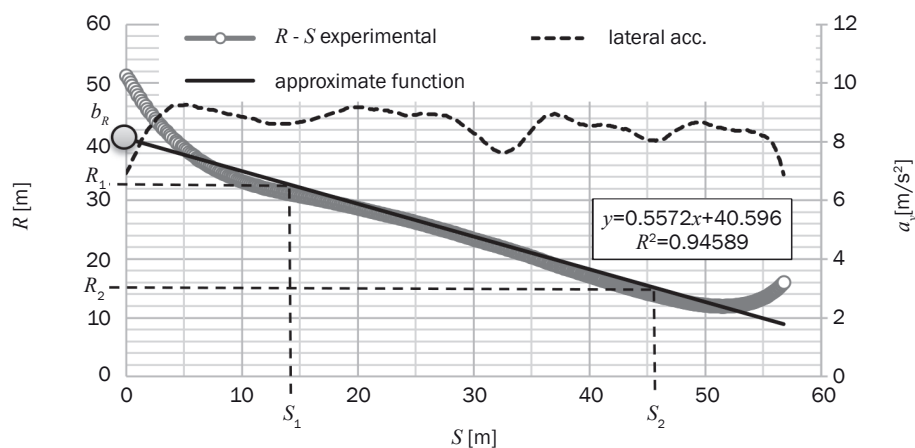

Figure 7 – The parameters of the trajectory radius change (the initial velocity v=16.22 m/s)
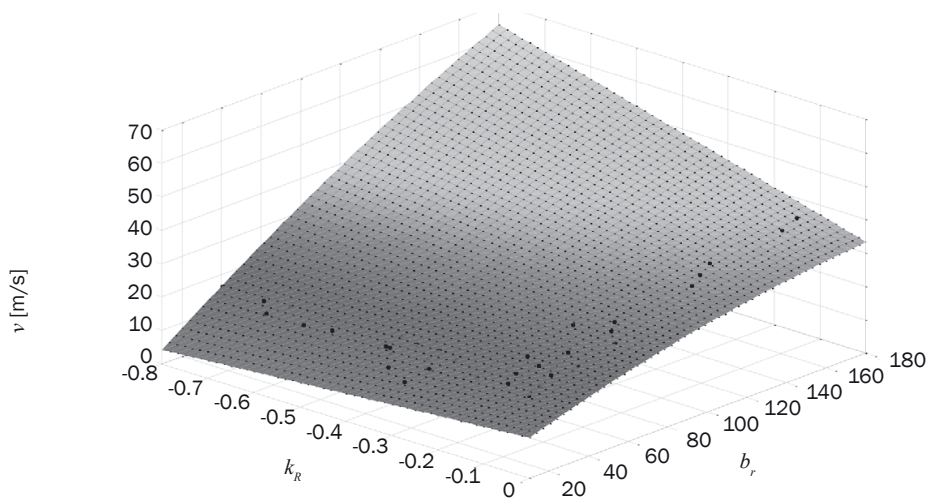
Figure 8 – The dependence of the initial velocity on the parameters of the trajectory radius changes

specific value of the initial velocity of the vehicle (*Figure 7*). The radius variation found in the middle part of the tire mark is characterized by two coefficients: namely, the direction coefficient k_R and the curve height coefficient b_R. According to trajectory radius R variation in the stable zone, coefficient k_R is found as follows:

$$k_R = \left(\frac{R_1 - R_2}{S_1 - S_2} \right) \qquad (39)$$

Coefficient b_R is the value R of the intersection of the prolonged linear function approximating the radius changes with the beginning of the tire mark (the vertical axis at the point S=0) (*Figure 7*). It conforms to the initial radius of the tire mark trajectory; however, as an inconformity of experimental values in this part (and at the end of slipping) attests, establishing the velocity according to the initial radius R values would not be accurate.

It is important to mention that when vehicle moves in the slip mode, lateral acceleration does not increase (*Figure 7*), because the tires do not generate the contact forces sufficient to maintain the desired trajectory.

Using the dependence between the trajectory radius and the tire mark found by the experimental tests and mathematical simulation, the relation of the coefficients k_R and b_R is formed:

$$v(k_R, b_R) = p_1 b_R^2 + p_2 k_R b_R + p_3 k_R^2 + p_4 b_R + p_5 k_R + p_6 \qquad (40)$$

The coefficients of the *relation 40* are provided in *Table 1*.

To describe the relation of k_R and b_R, 41 experimental data were used, and the inspection for errors was carried out under the conditions of 27 experimental tests (*Figure 8*). The relative error of 1.94% and the mean error of 0.395 were found between the real vehicle velocity in the beginning of tire mark formation and the velocity established on the basis of the coef-

Table 1 – The coefficients of the function describing the parameters of the trajectory radius changes

Coeff.	Value
p_1	−0.0004506
p_2	−0.2852
p_3	−0.1968
p_4	0.209
p_5	12.8
p_6	10.25

ficients describing the trajectory radius changes. Other parameters of conformity of the regression model: R^2 =0.993, SSE=309.22; $RMSE$=2.972.

For practical application of the developed methodology in traffic event investigations (predicting the initial vehicle velocity), photogrammetry and mathematical simulation should be combined and coordinated for use on a mutual platform:
- According to the parameters of the vehicle and the road conditions, mathematical simulation will form a typical dependence between the initial velocity and the slipping trajectory changes;
- Photogrammetry is useful for establishing the parameters of changes of a steady slipping trajectory.

5. CONCLUSIONS

In the paper, the initial or critical speed of a vehicle in the slip mode is analyzed. The yaw marks left by sideslipping tires on the road surface present one of the principal means of traffic event investigation. The mathematical simulation of vehicle movement provides an opportunity to carry out experimental tests that are difficult to accomplish in practice and considerably extends the scope of the investigation. In this paper, by applying the developed and experimentally validated mathematical model of a vehicle, the

dependence of vehicle velocity on slipping trajectory radius as well as on tire mark length was established. The experimental tests show that tire yaw marks are formed on dry asphalt pavement when lateral acceleration exceeds 0.7 m/s^2. The steadily changing middle part of a tire mark conforms to the regularities of a linear dependence, so the velocity of the vehicle in the initial phase of tire mark formation was related to the dependence according to the radius change direction coefficient and the curve height coefficient found by experiments and formed by the mathematical simulation. When the methodology is applied to other driving conditions, the expression for velocity determination should be more closely defined according to the validated mathematical model adapted for the parameters of the specific vehicle and the road conditions.

The obtained results and the formulated conclusions supplement modern methods for traffic event site fixation based on image fixing and processing technologies. If the data required for calculations are established by applying modern fixation systems and are related with models simulating the vehicle movement dynamics in an automated way, human data collection and processing errors will be minimized. The presented material is an optional tool for traffic accident researchers.

Dr. **VIDAS ŽURAULIS**[1]
E-mail: vidas.zuraulis@vgtu.lt
Prof. Dr. **EDGAR SOKOLOVSKIJ**[2]
E-mail: edgar.sokolovskij@vgtu.lt
[1] Transporto inžinerijos fakultetas
   Transporto ir logistikos kompetencijos centras
   Vilniaus Gedimino technikos universitetas
   Saulėtekio al. 11, LT-10223 Vilnius, Lietuva
[2] Transporto inžinerijos fakultetas
   Automobilių inžinerijos katedra
   Vilniaus Gedimino technikos universitetas
   J. Basanavičiaus g. 28, LT-03224 Vilnius, Lietuva

AUTOMOBILIO GREIČIO RYŠYS SU SLYDIMO TRAJEKTORIJOS KITIMU: TAIKYMAS EISMO ĮVYKIŲ TYRIMUI

SANTRAUKA

Straipsnyje nagrinėjamas posūkio trajektorija slydimo režimu judančio automobilio greičio ryšys su padangų slydimo pėdsakų parametrais. Tiriant eismo įvykius pradinis posūkyje išslydusio automobilio greitis nustatomas pagal padangų pėdsakų trajektorijos spindulį, kurio reikšmė praktikoje labai priklauso nuo tiesiogiai matuojamų pėdsako parametrų. Sudarytas ir eksperimentu validuotas 14 laisvės laipsnių automobilio matematinis modelis šiame darbe naudojamas slydimo trajektorijų tyrimui. Pradinio automobilio greičio priklausomybė nuo slydimo pėdsalo ilgio ir trajektorijos spindulio nustatyta kaip charakteringa, o pastovus slydimo dalį aproksimavus daugianariu, jo parametrais susieti su automobilio greičiu. Priklausomybės nustatytos tikrinant konkrečiais eksperimentiniais bandymais ir sudaryto modelio kompiuterine simuliacija.

RAKTINIAI ŽODŽIAI

automobilio greitis; slydimo trajektorija; automobilio modelis; eismo įvykis; šoninio slydimo pėdsakai;

REFERENCES

[1]   *CARE Database/EC*. Community Road Accident Database; 2012.

[2]   *Safety net accident causation database 2005 to 2008*. EC; 2010.

[3]   Žuraulis V, Sokolovskij E, Matijošius J. The opportunities for establishing the critical speed of the vehicle on research in its lateral dynamics. *Eksploatacja i Niezawodnosc – Maintenance and Reliability*. 2013;15(4): 312-318.

[4]   Muha R, Sever D. The impact of Regulation 561/2006 on fleet management viewed through efficient use of drivers' working time. *Promet – Traffic & Transportation*. 2009;21(1): 61-67.

[5]   Crisman B, Roberti B. Tyre wet-pavement traction management for safer roads. *Procedia - Social and Behavioral Sciences*. 2012;53: 1055-1068.

[6]   Brach RM. *An analytical assessment of the critical speed formula*. SAE Paper No. 970957; 1997.

[7]   Echaveguren T, Bustos M, Solminihac H. Assessment of horizontal curves of an existing road using reliability concepts. *Canadian Journal of Civil Engineering*. 2005;32(6): 1030-1038.

[8]   Franck H, Franck D. *Mathematical methods for accident reconstruction: a forensic engineering perspective*. Taylor & Francis Group, LLC; 2010.

[9]   Wach W. Structural reliability of road accidents reconstruction. *Forensic Science International*. 2013;228: 83-89.

[10] Wang YW, Wu J, Lin Ch N. A line-based skid mark segmentation system using image-processing methods. *Transportation Research Part C*. 2008;16: 390-409.

[11] Žuraulis V, Matuzevičius D, Serackis A. A method for automatic image rectification and stitching for vehicle yaw marks trajectory estimation. *Promet – Traffic & Transportation*. 2016;28(1): 23-30.

[12] Hoekwater J. *Traffic accident reconstruction. Participant guide*; 2008.

[13] Masory O, Gall EL, Bartlett W, Wright B. Experimental determination of the translational acceleration values for a spinning vehicle. In: *Proceedings of the Florida Conference on Recent Advances in Robotics, FCRAR 2006, 25 - 26 May 2006, Miami, Florida, USA*; 2006. p. 1-4.

[14] Seipel G, Winner H. *Development and intensity of tyre marks - analysis of influencing parameters*; 2013.

[15] Reif K. *Fundamentals of automotive and engine technology*. Springer Vieweg; 2014.

[16] Hirano Y, Inoue Sh, Ota J. Model-based development of future small EVs using modelica. In: *Proceedings of the 10th International Modelica Conference, 10 - 12 March 2014, Lund, Sweden*; 2014. p. 63-70.

[17] Sokolovskij E, Prentkovskis O. Investigating traffic accidents: the interaction between a motor vehicle and a pedestrian. *Transport*. 2013;28(3): 302-312.

[18] Shim T, Ghike Ch. Understanding the limitations of different vehicle models for roll dynamics studies. *Vehicle System Dynamics*. 2007;45(3): 191-216.

[19] Sulaiman S, Samin P M, Jamaluddin H, Rahman R A, Burhaumudin M S. Modeling and validation of 7-DOF ride model for heavy vehicle. In: *Proceedings of the International Conference on Automotive, Mechanical and Materials Engineering (ICAMME'2012), 19 - 20 May 2012, Penang, Malaysia*; 2012. p. 108-112.

[20] ISO 8855:2011. *Road vehicles. Vehicle dynamics and road-holding ability – Vocabulary*.

[21] ISO 8608:1995. *Mechanical vibration – Road surface profiles – Reporting of measured data*.

[22] Feng J, Zhang X, Guo K, Ma F, Karimi HR. A frequency compensation algorithm of four-wheel coherence random road. *Mathematical Problems in Engineering*. 2013; 1-12.

[23] Zhang Y, Chen W, Chen L, Shangguan W. Non-stationary random vibration analysis of vehicle with fractional damping. In: *Proceedings of the 13th National Conference on Mechanisms and Machines, 12 - 13 December 2007, Bangalore, India*; 2007. p. 171-178.

[24] Majdoub KE, Giri F, Ouadi H, Dugard L, Chaoui FZ. Vehicle longitudinal motion modelling for nonlinear control. *Control Engineering Practice*. 2012;20: 69-81.

[25] Jazar RN. *Vehicle dynamics: theory and application*. Springer Science+Business Media, LLC; 2008.

[26] Brach RM, Brach RM. *Tyre models for vehicle dynamic simulation and accident reconstruction*. SAE Paper No. 0102, 2009.

[27] Schramm D, Hiller M, Bardini R. *Vehicle dynamics: modeling and simulation*. Springer; 2014.

[28] Bogdevičius M. *Transporto priemonių dinamika: metodiniai praktinių uždavinių nurodymai*. Vilnius, Lietuva: Technika; 2012.

[29] Schiehlen W. *Dynamical analysis of vehicle systems. CISM courses and lectures*. Springer, Wien, NewYork; 2007.

[30] Pauwelussen J P. *Essentials of vehicle dynamics*. Butterworth-Heinemann, Elsevier Ltd; 2015.

[31] Corrsys-Datron. *Instruction manual*. A Kistler Group Company; 2012.